Geophysical Journal (1989) **96**, 131–138

A reinterpretation of the precursory seismic *b*-value anomaly from fracture mechanics

Ian G. Main
Department of Geology, University of Reading, Whiteknights, Reading RG6 2AB, UK

Philip G. Meredith and Colin Jones
Department of Geological Sciences, University College London, Gower Street, London WCIE 6BT, UK

Accepted 1988 July 5. Received 1988 June 17; in original form 1988 May 5

SUMMARY

A new model is presented which can explain the major temporal fluctuations in seismic *b*-value in terms of the underlying physical processes of time-varying applied stress and crack growth under conditions of constant strain rate. The model predicts two minima in the *b*-value, separated by a temporary maximum of inflexion point; a corollary being that a single broad maximum would be expected in scattering attenuation. These fluctuations in *b*-value are consistent with reported 'intermediate-term' and 'short-term' earthquake precursors separated by a period of seismic quiescence. We present preliminary results from controlled laboratory experiments and report recent field observations both of which are consistent with the predicted form, and in particular exhibit the distinctive, second short-term anomaly which reaches a value $b_c = 0{\cdot}5$ during the critical phase.

Key words: *b*-values, fracture mechanics, fractal dimension, earthquake precursors

INTRODUCTION

If earthquakes occurred as a simple process of elastic rebound following the build-up and release of tectonic strain energy, then it would be a simple matter to predict when the failure stress (σ_f) would be recovered, from the data of occurrence of a previous event and the observed rate of stress input (Shimazaki & Nakata 1980). However, in nature a period of precursory strain energy release in the form of brittle fracture by small earthquakes and tensile microcracking, sometimes coupled with aseismic crustal deformation, is commonly observed (Rikitake 1976; Mogi 1985). It is this period of anelastic deformation which gives rise to a plethora of intermediate-term and short-term earthquake precursors. Some of the most significant of these to date have been the spatial and temporal variations in seismicity statistics and wave propagation effects such as changes in seismic velocities and scattering attenuation (coda Q^{-1}) (Rikitake 1976, 1987). In particular, several authors (e.g. Smith 1981, 1986; Imoto & Ishiguro 1986) have cited changes in the seismic *b*-value (the slope of the log-linear frequency-magnitude relation) as an important, statistically significant precursor, and Jin & Aki (1980) have noted its correlation with scattering attenuation anomalies. This would be expected if the clusters of dilatant tensile microcracks thought to be responsible for time-dependent coda Q^{-1} variations are related spatially and temporally to precursory shear slip on subsidiary faults.

Variations in the seismic *b*-value have already been qualitatively linked to the state of stress (Scholz 1968); to changes in fracture mechanism (Meredith & Atkinson 1983) in laboratory-scale rock fracture experiments; and to the heterogeneity of the material (Mogi 1967). Here we present a new model, based on the principles of fracture mechanics and on results from earlier laboratory experiments. This model, first presented in Main & Meredith (1987), can explain qualitatively the major temporal fluctuations in *b*-value in terms of the underlying physical processes of time-varying applied stress and crack growth under conditions of constant strain rate, and also predicts quantitatively the observed critical *b*-value of 0·5 found during foreshock sequences.

FRACTURE MECHANICS MODEL

In this section we develop a model based on earlier laboratory observations of precursory microcracking in stressed rock samples. We consider two models of stress–time behaviour, which we shall term Model (1)—elastic failure (time-predictable model) and Model (2)—anelastic failure (involving precursory strain energy release). The geologically most apt boundary condition is a constant rate of remotely applied strain, so time and remote strain are equivalent parameters in this discussion. Where there is precursory anelastic deformation, the rock continues to support a high but decreasing level of stress for some time after the peak stress has been achieved, and before

catastrophic failure occurs. Such strain softening is a common feature observed in the laboratory (e.g. Paterson 1978), and it is also commonly invoked in the geological literature to explain strain fabrics in shear zones (e.g. White *et al.* 1980). Several mechanisms have been proposed to explain this precursory reduction in differential effective stress prior to earthquakes: dilatancy hardening followed by an increase in pore fluid pressure in the fault nucleation zone (Scholz, Sykes & Aggarwal 1973); strain softening caused by crack coalescence (dry dilatancy: Miachkin *et al.* 1972), or slip weakening where a fault exists (Stuart 1979).

The observation that catastrophic failure commonly occurs below the peak stress can be explained by invoking the concept of fracture mechanics, where the crucial parameter is the resistance to fracture rather than the level of applied stress. The most useful measure of this resistance for our purposes is the stress intensity factor, $K = Y\sigma\sqrt{X}$, as defined by Lawn & Wilshaw (1975). σ is the level of remotely applied stress, X is the length of the propagating crack or flaw, and Y is a known geometric factor which has been tabulated for a wide range of crack configurations (e.g. Sih 1973). Thus the crucial parameter governing dynamic fracture is dependent on both the level of applied stress and the crack length. However, even below the critical value of K for catastrophic mechanical rupture (i.e. the fracture toughness, K_c), stable, subcritical crack extension primarily due to chemically enhanced stress corrosion reactions can still take place over a continuous range of values of K (Atkinson & Meredith 1987a). The crack extension velocity is found experimentally to be related to the stress intensity according to Charles' law, $\dot{X} = A \cdot K^n$, where A is a constant and n is known as the stress corrosion index. n is generally found to be in the range $20 < n < 60$ for earth materials (Atkinson & Meredith 1987b) so the acceleration from quasi-static (subcritical) to dynamic (critical) fracture is highly non-linear but nevertheless not an instantaneous process. For the case of constant stress (Das & Scholz 1981), it can be shown that

$$X/X_0 = (1 - t/t_f)^{2/(2-n)}, \tag{1}$$

where t_f is the dynamic failure time and X_0 is the initial crack length at time $t = 0$. For the more general condition of a time-varying stress (Main 1988) the functional form of equation (1) still holds to a very good approximation (i.e. better than 2 per cent in X), although failure occurs earlier than for a constant stress. This holds because the stress increase between earthquakes and subsequent stress drop (order of 30 bars) is usually only a small fraction of the residual frictional stress (order of 1 kbar at shallow seismogenic depths). The failure time is then given to a reasonable approximation by

$$t_f = (X_0/V_0)[2/(n-2)]/(1 + n\,\Delta\sigma/2\sigma_0), \tag{2}$$

where $\Delta\sigma$ is the potential stress drop built up from an initial level of σ_0, equivalent to the static frictional stress, and V_0 is the initial crack extension velocity at time t_0. Since the stress drop during earthquakes is generally only a small fraction of σ_0, equation (2) demonstrates that, to first order at least, the crack grows independently of the additional stress built up between earthquakes, in a manner analogous to static fatigue encountered in engineering. However, the reverse is not true, since precursory crack extension and the resulting slip behind the crack tip can have a marked influence on $\Delta\sigma$, particularly near to catastrophic failure, and a full treatment of the dynamic phase would require a constitutive relation between strain release and stress drop.

Figure 1 illustrates the temporal variations in stress, crack length, stress intensity and the observed seismic b-value predicted from the above theory for Models (1) and (2). These diagrams are schematic rather than rigorously quantitative, since the anelastic deformation phase of the earthquake cycle is not thought to exceed a few percent of the recurrence time of major earthquakes (Rikitake 1987). In order to model the shape of the b-value anomaly, it is necessary to use an empirical relationship between b and K established from laboratory acoustic emission data (Meredith & Atkinson 1983). We make qualitative use of this relationship even though it was obtained from tensile crack propagation experiments, because there appears to be no good physiochemical reason why the functional form of the time dependent stress corrosion process should depend on the mode of fracture, and similar data are not yet available for shear modes. Das & Scholz (1981) justify this assumption on the basis that rocks in compression under high pressure exhibit dilatant creep and static fatigue, both processes that result from stress corrosion. Furthermore, in their experimental study of shear rupture, Cox & Scholz (1988) noted that the growth of macroscopic shear ruptures was dominated by the development of arrays of tensile microcracks at least in its early stages, and hence the long-term behaviour of shear fractures should be controlled by the same time-dependent processes as tensile cracks. The form of this relationship is

$$b = p - qK, \tag{3}$$

where $\log N = a - bM$, and a, p and q are empirical constants. M is earthquake magnitude or the analogous acoustic emission amplitude (in dB), and N can be a discrete or cumulative frequency.

Figure 1(a) shows the stress–time behaviour of the two models. Model (1) has a monotonic increase in stress from an initial stress σ_0 at time t_0 until failure at peak stress σ_f at the failure time t_{f_1}. Model (2) by contrast exhibits both strain-hardening and strain softening anelastic phases, with quasi-static failure occurring at the peak stress before dynamic failure at time t_{f_2}. Fig. 1(b) shows the temporal form of the crack extension from an initial length X_0 at time t_0 to effectively infinite values at time t_f.

Figure 1(c) shows the combined effects of stress and crack length on the stress intensity factor K, showing quite complicated behaviour for Model (2). K increases gradually from a value K_0 at time t_0 to a level approaching the fracture toughness K_c, when a precursory decrease in stress (Fig. 1a) at first reduces K temporarily before the effect of the accelerating crack begins to dominate K (Fig. 1b; model 2), causing a rapid increase to critical failure. If slip-weakening due to crack growth is the dominant mechanism of stress reduction, then an inflexion rather than a first maximum in K would be expected (Fig. 1a,b,c; dashed lines), since such slip-weakening would increase the stress intensity during the strain softening phase by concentrating stress at the crack tip. After the earthquake, at time t_{f_2}, K once again reduces to a residual level K_0.

Figure 1(d) shows the form of the b-value anomaly expected if b is inversely correlated to K as demonstrated by Meredith & Atkinson (1983). This diagram is the only section of Fig. 1 which has a quantitative scale on the vertical axis, showing that we would expect b to vary between 0·5 and 1·5 during the earthquake cycle, and that critical failure in a large earthquake should occur at $b_c = 0{\cdot}5$. Main (1988) has shown that this can be demonstrated theoretically to be a consequence of the critical coalescence of neighbouring microcracks and Von Seggern (1980) has tabulated a number of empirical observations of foreshock sequences with a mean b-value of 0·51 and a standard deviation of 0·10.

By contrast the experiments of Meredith & Atkinson (1983) show b to be in the range 1–3, with $b_c = 1$. In order to explain this apparent discrepancy, it is necessary to

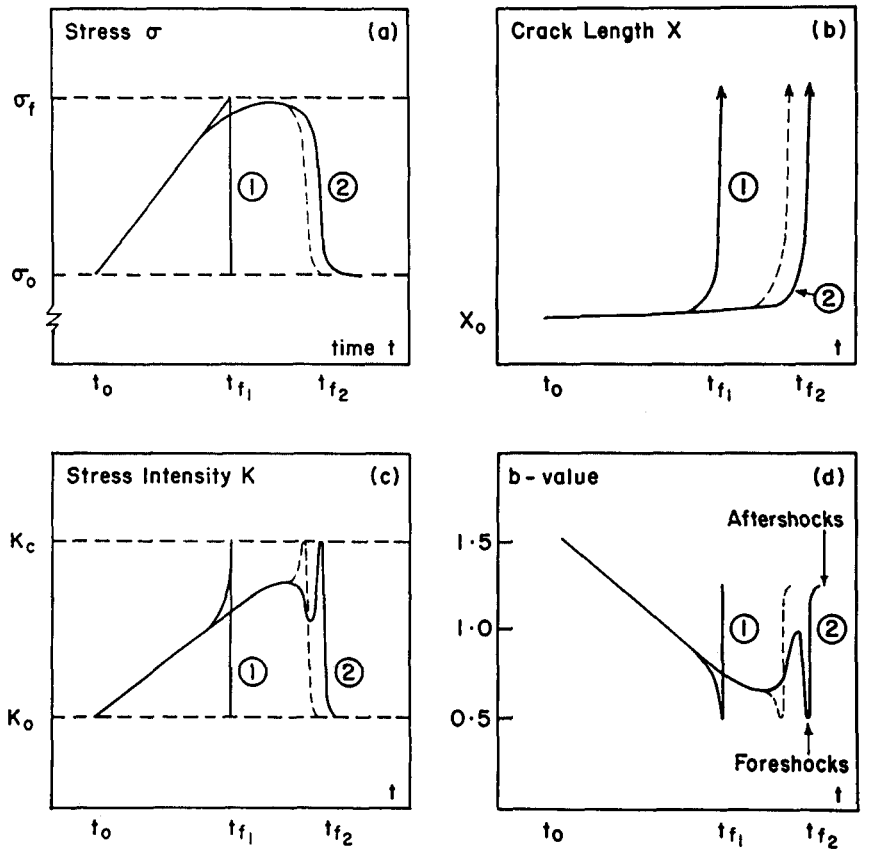

List of variables

① Model 1 : Elastic failure

② Model 2 : Anelastic failure

σ_o Initial stress at time t_o

σ_f Nominal failure stress (peak stress)

t_o Onset time of loading

t_{f_1} Dynamic failure time for Model 1

X_o Crack length at time t_o

t_{f_2} Dynamic failure time for Model 2

K_o Stress intensity at time t_o

K_c Critical stress intensity (fracture toughness)

Figure 1. Fracture mechanics models of the b-value anomaly for Model (1): elastic failure (time-predictable model) and Model (2): anelastic failure (precursory strain energy release). (a) Time dependence of the level of stress. Note that for model (2) the dynamic failure stress is *lower* than the peak stress. (b) Acceleration of crack tip to critical failure by stress corrosion. The dashed line is an intermediate case where acceleration to critical rupture velocities occurs earlier in the cycle. (c) Combined effect of (a) and (b) on the stress intensity factor. An earlier phase of crack growth (dashed line) leads to an inflexion rather than a temporary reduction in K. (d) Since b is negatively correlated and linearly related to K, all models predict a decreasing b-value over most of the seismic cycle, but only model (2) predicts an intermediate-term phase of increasing b-value. Note that the forms shown are qualitative only, though the critical b-value is $b_c = 0.5$, and $0.5 \leq b < 1.5$.

invoke a dislocation model of the earthquake source (Kanamori & Anderson 1975), and consider the distribution of earthquake magnitudes resulting from a power law distribution of fault lengths. If the discrete length distribution (of faults or microcracks) is a power law of negative exponent D, then it can be shown that $b = cD/3$ (Caputo 1976), where c is a constant equivalent to the slope of the log-linear moment–magnitude relation (Kanamori 1978).

For the experiments cited (Meredith & Atkinson 1983), $c = 3$ for a simple dislocation model (see Appendix), and therefore the critical value of D is unity for $b_c = 1$. Thus to scale the b-values determined from these laboratory experiments to typical earthquakes, we have to take account of the fact that $c = 1{\cdot}5$ for intermediate and large earthquakes (Kanamori & Anderson 1975; Kanamori 1978). The scaled-up critical b-value for large earthquakes for $D_c = 1$ would be $b_c = 0{\cdot}5$, which is within the observed range of 0·35–0·61 for foreshocks of several major events (Von Seggern 1980). There is also support for this from laboratory studies where b_c is found to be in the range 0·3–0·5 (Weeks, Lockner & Byerlee 1978), and the results presented here (Figs. 2 and 3) are further confirmation of this prediction. This astonishing consistency between laboratory and field observation is a strong justification for adopting a scale-invariant power law distribution of faults or microcracks. Note that the crucial parameter is not b, which also depends on the relative time constants of the event and recording instruments, but D, which depends only on the geometry of the system of faults or microcracks. It can also be shown (Main 1988) that the average crack length becomes unstable where $D_c = 1$, analogous to a critical mean free path problem. A physical interpretation of this is the critical coalescence of neighbouring microcracks to produce one major dynamic event. For the special case of a scale-invariant distribution of faults or cracks with, in general, a non-integer exponent, D is equivalent to the fractal dimension of the system (Mandelbrot 1982).

Thus Fig. 1(d) shows the model predictions for the shape of the b-value anomaly expected in earthquake zones. For earthquakes with few foreshocks it may not always be possible to discern with sufficient statistical significance the distinctive and relatively short-term dip in b-value. The period of decreasing stress prior to rupture, which causes the temporary lowering of K and the corresponding increase in b-value, could also be responsible for the phenomenon of precursory quiescence (Wyss 1986) which is often associated with an increasing b-value (Smith 1981, 1986). However, the major intermediate-term feature of the b-value anomaly for precursory deformation is a convex-downward decrease to a minimum above the critical value of 0·5, followed by a recovery, or at least an inflexion. Elastic deformation would produce a monotonic concave-downward decrease. The two dips in the b-value for the former case may be linked to the two major classes of precursor defined as intermediate-term and short-term (Rikitake 1976; Mogi 1985; Main & Meredith 1988).

By contrast, the resultant effect of the growth of such precursory cracks and faults on scattering attenuation (coda Q^{-1}) may be to produce only one broad maximum, since coda Q^{-1} responds to the *cumulative* production by fracturing of additional scatterers in the earth, rather than the contemporary distribution sampled by the b-value.

LABORATORY AND FIELD RESULTS: DISCUSSION

Results from one of a series of laboratory-scale experiments designed to test the precursory strain energy release model by contemporaneous monitoring of deformation behaviour and seismic signals are illustrated in Fig. 2. The experimental arrangement is described in detail in Meredith, Main & Jones (1988), which includes laboratory failure under a wider range of conditions than discussed here, and also demonstrates that the results of Fig. 2 are reproducible. Fig. 2(a) shows the stress–time curve for a specimen of Darley Dale sandstone deformed in triaxial compression at nominally constant strain rate. This material was chosen specifically because it exhibited distinct phases of strain hardening and strain softening prior to dynamic shear rupture at the strain rates typical of laboratory experiments (10^{-4} to $10^{-6}\,s^{-1}$). This form of stress–time behaviour would also be expected for crystalline rocks (granitic, basaltic) present at earthquake nucleation depths but at slower, geologically more realistic strain rates ($\sim 10^{-14}\,s^{-1}$). The peak stress is followed by a significant precursory decrease in stress prior to unstable failure on a well-defined fault plane and, finally, stable sliding along the fault (Fig. 2a). Contemporaneous acoustic emission rate data are shown in Fig. 2(b). Note the rapid acceleration of acoustic emission rate associated with the onset of microcracking indicated by a deviation from linearity of the stress–time curve preceding the peak stress. After peak stress, the rate at first flattens out and then falls dramatically to a period of apparent quiescence, but then recovers immediately following instability in a manner analogous to an aftershock sequence. (Instability is marked by a pronounced minimum in acoustic emission rate due to smaller events running into each other to produce one major dynamic event, consistent with the assumption of critical crack coalescence at dynamic rupture.)

Temporal variations in the b-value, derived by the maximum likelihood method (Aki 1965) from the data of Fig. 2(b), show all of the features predicted by the intermediate model (Fig. 1d; dashed line). The major trend is of a decreasing b-value, correlated with increasing stress, which flattens out around peak stress ($\dot{b} > 0$), and constrasts sharply with the cusp-like anomaly expected for the time-predictable model ($\dot{b} < 0$). This phase is followed by an inflexion point leading to a much shorter time-scale, foreshock-related b-value anomaly of about 0·5. (For this triaxial compression experiment, $c = 1{\cdot}5$, so again the critical fractal dimension is unity—see Appendix.) Post-failure the b-value recovers as expected. Thus the broad pattern of this anomaly is exactly as expected if acceleration of fracture and slip-weakening are the dominant mechanisms of post-peak stress reduction. Since there is no intermediate-term decrease in stress intensity for this model, no marked precursory quiescence phase is expected or observed. Note also that there is no simple, direct, inverse correspondence between stress level and b-value as has previously been suggested (Scholz 1968); the pattern is more complicated and depends also on whether the stress level is increasing or decreasing.

Further evidence in support of the model comes from a recent study (Imoto & Ishiguro 1986) of temporal changes in the b-value preceding the Western Nagano, Japan,

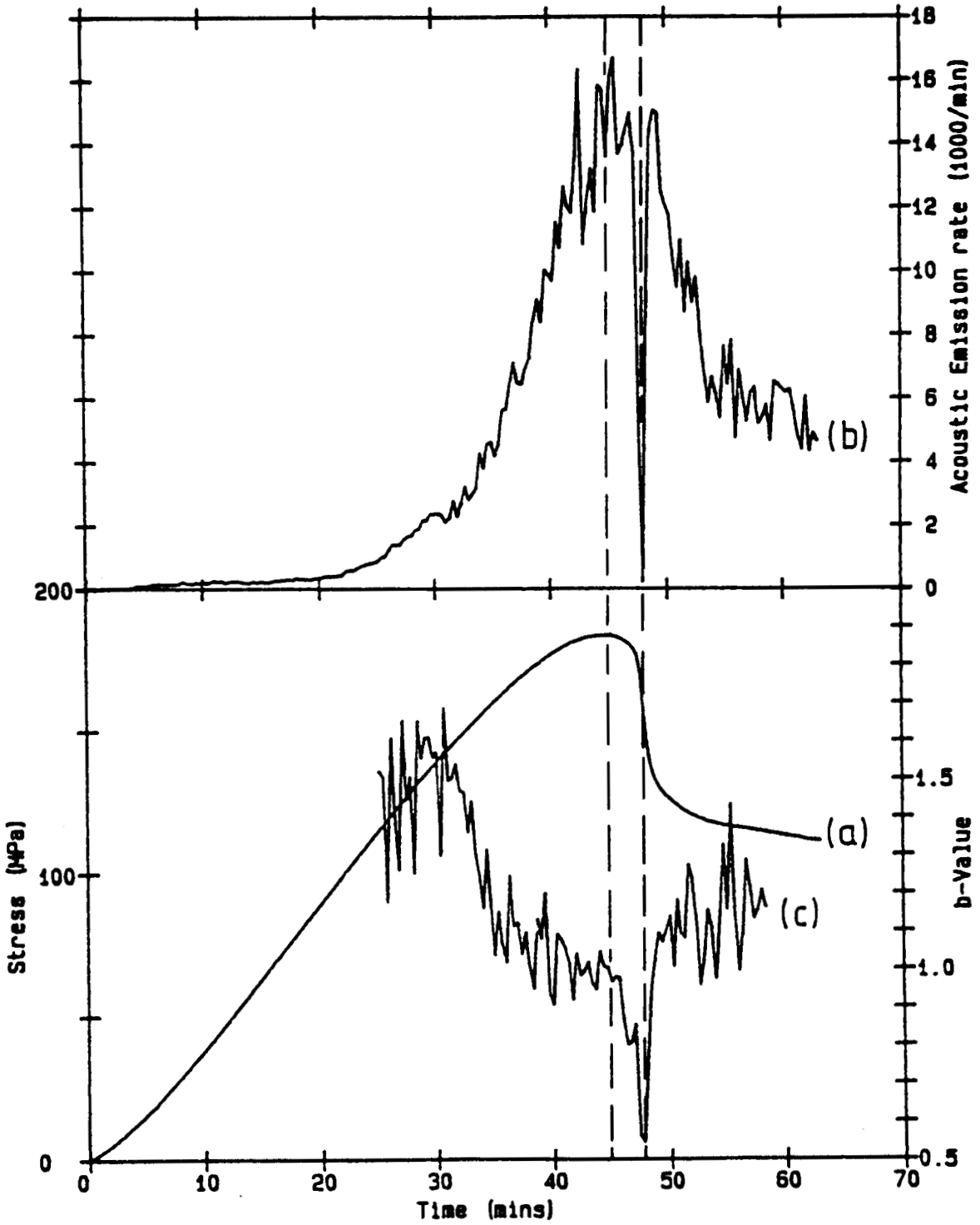

Figure 2. Contemporaneous measurements of (a) differential stress, (b) acoustic emission rate and (c) b-value as functions of time for a water-saturated sample of Darley Dale sandstone deformed at a constant strain rate of $2 \times 10^{-5}\,s^{-1}$ under a confining pressure of 50 MPa. (a) The differential stress–time curve is markedly non-linear with significant post-peak stress decrease prior to unstable faulting and stable sliding. (b) The acoustic emission rate increases rapidly during a period of microcracking prior to peak stress. The rate at first flattens out, and then falls dramatically after peak stress to a period of apparent quiescence at dynamic failure. Recovery immediately following instability may be associated with aftershocks. (c) A decreasing b-value associated with increasing stress leads to a broad flattening at peak stress followed by an inflexion and then a short-term low b-value anomaly at failure. This is exactly the form predicted by the dashed-line in Fig. 1(d) and is in good agreement with the quantitative prediction $0.5 \leqslant b < 1.5$ and $b_c = 0{\cdot}5$. Post-failure the b-value recovers.

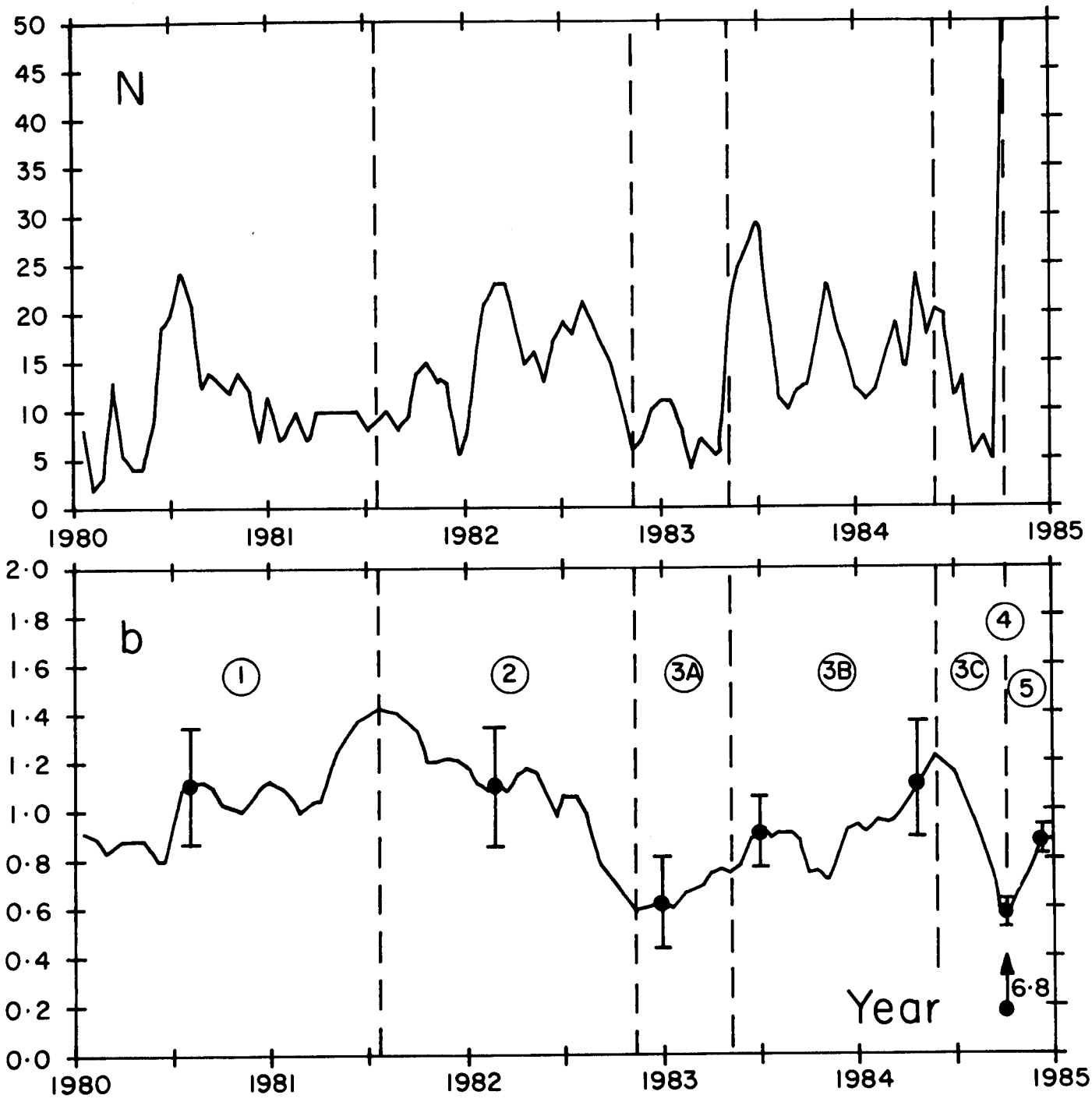

Figure 3. Temporal variation in the number of seismic events N and in the b-value measured for the Western Nagano, Japan, earthquake ($M_s = 6{\cdot}8$) of 1984 September, after Imoto & Ishiguro (1986). The data show clearly both the intermediate-term and short-term b-value anomalies predicted by model (2), though the error bars at selected points of the curve show that the $b_c = 0.55 \pm 0.02$, obtained from 493 events, is the most statistically significant feature. The diagram is split into phases 1 (elastic stress build up), 2 (strain hardening), 3 (strain softening), 4 (dynamic failure) and 5 (aftershocks) according to Model (2) of Fig. 1, as discussed in more detail in Main & Meredith (1988). Phase 3A is thought to be dominated by crack coalescence, phase 3B by fluid diffusion and phase 3C by acceleration of fracture. Note that phases 3A and 3C are relatively quiescent, and that the phase thought to be dominated by fluid penetration into the nucleation zone is relatively active.

earthquake of September 14 1984 ($M_s = 6.8$). The data are reproduced in Fig. 3 with error estimates added at selected points, and show clearly the predicted intermediate-term and short-term b-value anomalies, though the level of statistical significance is much less marked than for the laboratory data. The pronounced recovery in the b-value between the winter of 1982 and the spring of 1984, similar to Smith's (1981, 1986) observation of precursory increase in b-value, indicates that this earthquake was preceded by a significant reduction in effective stress by a mechanism other than slip-weakening, perhaps due to diffusion of pore fluids. Smith (1986) also noted several examples of a short-term drop in b-value after an intermediate-term rise, and noted that the relative durations of these phases was generally in the ratio 1:4. For Fig. 3 this ratio is found to be 1:4·7, showing consistency with Smith's results. The diagram also indicates that outside controlled laboratory conditions there is the possibility of transient stress changes caused by neighbouring faults, which can give rise to significant statistical fluctuations and hence to possible false alarms. This paper shows that the b-value anomaly may be a good indicator of the current level of stress intensity, but it should never be used on its own to issue a high-level earthquake warning.

ACKNOWLEDGMENTS

We thank Masajiro Imoto and Makio Ishiguro for generously providing their original data required for Fig. 3. Financial support for this work was provided in part by the British Natural Environment Research Council through research grant GR3/6293.

REFERENCES

Aki, K., 1965. Maximum likelihood estimate of b in the formula $\log N = a - bm$ and its confidence limits, *Bull. Earthq. Res. Inst. Tokyo Univ.*, **43**, 237–239.

Atkinson, B. K. & Meredith, P. G., 1987a. The theory of subcritical crack growth and its application to minerals and rocks, in *Fracture Mechanics of Rock*, pp. 111–166, ed. Atkinson, B. K., Academic Press, London.

Atkinson, B. K. & Meredith, P. G., 1987b. Experimental fracture mechanics data for rocks and minerals, in *Fracture Mechanics of Rock*, pp. 477–525, ed. Atkinson, B. K., Academic Press, London.

Caputo, M., 1976. Model and observed seismicity represented in a two-dimensional space, *Ann. Geophys. (Rome)*, **4**, 277–288.

Cox, S. J. D. & Scholz, C. H., 1988. Rupture initiation in shear fracture of rocks: an experimental study, *J. geophys. Res.*, **93**, 3307–3320.

Das, S. & Scholz, C. H., 1981. Theory of time-dependent rupture in the earth, *J. geophys. Res.*, **86**, 6039–6051.

Imoto, M. & Ishiguro, M., 1986. A Bayesian approach to the detection of changes in the magnitude-frequency of earthquakes, *J. Phys. Earth*, **34**, 441–445.

Jin, A. & Aki, K., 1980. Temporal change in coda Q before the Tangshan earthquake of 1976 and the Haicheng earthquake of 1975, *J. geophys. Res.*, **91**, 665–673.

Kanamori, H., 1978. Quantification of earthquakes, *Nature*, **271**, 411–414.

Kanamori, H. & Anderson, D. L., 1975. Theoretical bases of some empirical relations in seismology, *Bull. seism. Soc. Am.*, **65**, 1073–1095.

Lawn, B. R. & Wilshaw, T. R., 1975. *Fracture of Brittle Solids*, Cambridge University Press, Cambridge.

Main, I. G., 1988. Prediction of failure times in the Earth for a time-varying stress, *Geophys. J.*, **92**, 455–464.

Main, I. G. & Meredith, P. G., 1987. A reinterpretation of the seismic b-value anomaly from fracture mechanics, in Proc. *XIX General Assembly of the International Union of Geodesists and Geophysicists*, Vancouver, Canada (abstract), vol I, p. 260.

Main, I. G. & Meredith, P. G., 1988. Classification of earthquake precursors from a fracture mechanics model, *Tectonophys.*, in press.

Mandelbrot, B. B., 1982. *The Fractal Geometry of Nature*, Freeman, San Francisco.

Meredith, P. G. & Atkinson, B. K., 1983. Stress corrosion and acoustic emission during tensile crack propagation in Whin Sill dolerite and other basic rocks, *Geophys. J.R. astr. Soc.*, **75**, 1–21.

Meredith, P. G., Main, I. G. & Jones, C., 1989. Temporal variations in seismicity during quasi-static and dynamic rock failure, *Tectonophys.*, in press.

Miachkin, V. I., G. A. Sobolev, N. H. Dolbilkina, V. N. Morozov & Preobrazensky, V. B., 1972. The study of variations in geophysical fields near focal zones of Kamchatka, *Tectonophysics*, **14**, 287.

Mogi, K., 1967. Earthquakes and fractures, *Tectonophys.*, **5**, 35–55.

Mogi, K., 1985. *Earthquake Prediction*, Academic Press, London.

Paterson, M. S. 1978. *Experimental Rock Deformation—The Brittle Field*, Springer, Berlin.

Rikitake, K., 1976. *Earthquake Prediction, Developments in Solid Earth Geophysics, Vol.* **9**, Elsevier, Amsterdam.

Rikitake, K., 1987. Earthquake precursors in Japan: precursor time and detectability, *Tectonophys.*, **136**, 265–282.

Scholz, C. H., 1968. The frequency-magnitude relation of microfracturing in rock and its relation to earthquakes, *Bull. seism. Soc. Am.*, **58**, 399–415.

Scholz, C. H., Sykes, L. R. & Aggarwal, Y. P., 1973. Earthquake prediction: a physical basis, *Science*, **181**, 803–810.

Shimazaki, K. & Nakata, T., 1980. Time-predictable recurrence model for large earthquakes, *Geophys. Res. Letts.*, **7**, 279–282.

Sih, G. C., 1973. *Handbook of Stress Intensity Factors for Researchers and Engineers*, Institute of Fracture and Solid Mechanics, Lehigh University, Bethlehem.

Smith, W. D., 1981. The b-value as an earthquake precursor, *Nature*, **289**, 136–139.

Smith, W. D., 1986. Evidence for precursory changes in the frequency-magnitude b-value, *Geophys. J. R. astr. Soc.*, **86**, 815–838.

Stuart, W. S., 1979. Strain softening prior to two-dimensional strike-slip earthquakes, *J. geophys. Res.*, **84**, 1063–1070.

Von Seggern, D., 1980. A random stress model for seismicity statistics and earthquake prediction, *Geophys. Res. Letts.*, **7**, 637–640.

Weeks, J., Lockner, D. & Byerlee, J., 1978. Change in b-values during movement on cut surfaces in granite, *Bull. seism. Soc. Am.*, **76**, 333–341.

White, S. H., Burrows, S. E., Carreras, J., Shaw, N. D. and Humphreys, F. J., 1980. On mylonites in ductile shear zones, *J. struct. Geol.*, **2**, 175–187.

Wyss, M., 1986. Seismic quiescence precursor to the 1983 Kaoki ($M_s = 6·6$) Hawaii, earthquake, *Bull. seism. Soc. Am.*, **76**, 785–800.

APPENDIX: SCALING OF THE MOMENT-MAGNITUDE RELATION

The scalar seismic moment of an earthquake is defined as

$$M_0 = \mu A u, \tag{A1}$$

where u is the average slip on a fault of area A and μ is the rigidity modulus. It can be related to the magnitude M by the formula

$$\log M_0 = cM + d \tag{A2}$$

where c and d are empirical constants (Kanamori 1978).

Kanamori & Anderson (1975) showed that $c = 3$ when the following conditions hold

$$\tau > T_0/\pi; \qquad L/V > T_0/\pi \tag{A3}$$

where τ is the rise time of the event, L is the fault length, V the rupture velocity and T_0 is the natural period of the recording instrument. Under these conditions the instrument saturates because the corner frequency of the event is below its natural frequency.

For the tensile fracture experiments of Meredith & Atkinson (1983) 250 kHz transducers with $T_0 = 4\,\mu$s were used to record acoustic emissions with near-sonic rupture velocities of the order $1\,\mathrm{km\,s^{-1}}$. For an event of similar duration to the instrument period, this would correspond to microcrack sizes of the order 1 mm, similar to the grain size of the rocks in these tests and the dimensions of the microcracks revealed by reflection microscopy. Since most events are preceded by subcritical rupture propagation, V is likely to be an upper bound, so that $L/V > T_0/\pi$ holds except for a few abnormally dynamic small events. If the rise time τ is comparable to L/V, we would expect both conditions of (A3) to hold, and therefore $c = 3$ in (A2), and if

$$b = cD/3 \tag{A4}$$

(Caputo 1976), then $1 < b < 3$ would be expected if the microcracks were confined to a volume ($D < 3$) and the average crack length is to remain finite ($D > 1$; Main 1988). (Kanamori & Anderson (1975) showed that $L/V \sim 10\tau$, so the conditons holding in these experiments are likely to be $\tau \gtrsim T_0/\pi$; $L/V > T_0/\pi$).

By contrast the compressional failure experiment whose results are shown in Fig. 2 would be expected to have acoustic emissions with sharper onsets and shorter durations due to the relatively higher nucleation and fracture velocities produced by compression. Under these conditions it is more likely that

$$\tau \lesssim T_0/\pi; \qquad L/V \gtrsim T_0/\pi. \tag{A5}$$

If these conditions hold, the dislocation model of Kanamori & Anderson (1975) predicts $c = 1.5$, or $0.5 < b < 1.5$ for $1 < D < 3$. This is exactly what is found in Fig. 2 (compressional laboratory experiment with failure by shear faulting) and in field observation of earthquake statistics (e.g. Fig. 3).